Nanoemulsion preparation by combining high pressure homogenization and high power ultrasound at low energy densities

Energy density reduction for nanoemulsion preparation by combining high pressure homogenization and high power ultrasound

Sonia Calligaris[1], Stella Plazzotta[1], Francesca Bot[1], Silvia Grasselli[2], Annalisa Malchiodi[2], Monica Anese[1]*

[1]Dipartimento di Scienze degli Alimenti, Università di Udine, via Sondrio 2/A, 33100 Udine, Italy

[2]GEA Mechanical Equipment Italia S.p.A., Via A.M. Da Erba Edoari 29, 43123 Parma, Italy

* Corresponding author. Tel. +39 0432 558153; fax: +39 0432558130. *E-mail address*: monica.anese@uniud.it (M. Anese).

Abstract

Combinations of high pressure homogenization (HPH) and ultrasound (US) were studied as alternative processes to individual HPH and US to produce stable nanoemulsions, while reducing the energy requirement. A 15% oil-in-water mixture was homogenized by means of combinations of HPH and US. In particular, 20 to 100 MPa HPH was applied before or after 20 or 60 s US, providing low and medium energy densities. Emulsions were analyzed for particle size distribution and mean diameter, viscosity and physical stability. Results were compared with those relevant to emulsions prepared by the application of individual HPH and US, providing comparable or higher energy densities. US and HPH applied in combination at low and medium energy density values allowed to obtain nanoemulsion having lower mean particle dimensions and, in most cases, higher stability than those prepared by using individual US or HPH at high energy densities. A greater efficiency was found for US preceding HPH.

Keywords: Energy density reduction, High pressure homogenization, High power ultrasound, Nanoemulsion, Particle size

1. Introduction

High pressure homogenization (HPH) and high power ultrasound (US) induced changes of some physical and chemical properties of molecules are under study for exploitation at the industrial level for food processing and preservation purposes (Anese, Mirolo, Beraldo, & Lippe, 2013; Barba, Grimi & Vorobiev, 2015; Donsì, Annunziata, & Ferrari, 2013; Fathi, Martin, & McClements, 2014; Floury, Desrumaux, & Legrand, 2002; Huang, Hsu, Yang, & Wang, 2013; Panozzo et al., 2013; Patrignani et al., 2013; Rastogi, 2011). Moreover, HPH and US have been proposed as alternative techniques to produce nanoemulsions (10-100 nm radius) since they can impart a sufficiently high energy input to reduce the droplet dimensions at nano-level of oil-in-water mixtures (Canselier, Delam, Wihelm, & Abismaïl, 2002; Abbas, Hayat, Karangwa, Bashari, & Zhang, 2013; Dumay, Chevalier-Lucia, Benzaria, Gracià-Julià, & Blayo, 2013; McClements, 2005; Silva, Cerqueira & Vicente, 2012). The mean droplet diameter of an emulsion can be described as a function of energy density (E_v), that is the energy input per unit volume, by a power law (Stang, Schuchmann, & Schubert, 2001; Schubert, Ax, & Behrend, 2003). Thus, the greater the emulsification efficiency the lower the droplet diameter. The efficiency of HPH to generate nanoemulsions mainly depends on the geometry of the homogenization valve, while in the US systems cavitation is the main effect. In HPH, the fluid is forced to pass in few seconds through a narrow gap in the homogenization valve, where it is submitted to a rapid acceleration (Floury, Bellettre, Legrand, & Desrumaux, 2004; Floury, Legrand, & Desrumaux, 2004). The resulting pressure drop simultaneously generates intense mechanical forces, elongation stresses, cavitation and turbulence in the medium (Freudig, Tesch, & Schubert, 2003). Pressures between 50 and 150 MPa are generally applied to a coarse primary emulsion (Dumay et al., 2013; Solans, Izquierdo, Nolla, Azemar, & Garcia-Celma, 2005). During single pass process, a progressive decrease of the particle size can be obtained by increasing the homogenization pressure. However, up to a certain pressure level, which depends on the equipment design, particle size reduction is no more longer expected (Floury, Desrumaux, & Lardères, 2000; Dumay et al., 2013; Jafary, He & Bhandari, 2006; Lee & Norton, 2013; Quian & McClements, 2011). Multiple passes

through the homogenizer are eventually applied to further reduce not only the mean particle diameter but also the width of the particle size distribution, and improve emulsion stability against coalescence (Cortès-Munos, Chevaller, & Dumay, 2009; Floury et al., 2000; Quian & McClements, 2011). As a consequence an increase of energy requirement, that is proportional to the number of passes in the homogenizer, has to be expected.

In US, the energy is transferred to the fluid by the propagation of ultrasound waves in the frequency range of 20-100 kHz for a few seconds to several minutes (Abbas et al., 2013). These waves create alternate zones of compression and rarefaction, leading to development and subsequent collapse of microscopic cavitation bubbles. During collapse, intense shockwaves are created into the fluid, which are associated with high velocity gradients and shear stress. US emulsification is believed to occur mainly in the vicinity of the collapsing bubbles, where the high fluid velocity causes the mixing of emulsion and droplet size reduction (Ashokkumar, 2011). The longer the treatment time the greater the droplet break-up (Abbas et al., 2013; Delmas et al., 2011), up to a threshold above which a further increase in residence time would not lead to a concomitant reduction of droplet diameter (Kentish et al., 2008; Leong, Wooster, Kentish, & Ashokkumar, 2009).

It is noteworthy that the application of HPH and US for nanoemulsion preparation at the industrial level is limited by several drawbacks. One major issue is relevant to high energy requirement to generate nanoemulsions. This implies the use of specially designed equipment, working at high pressures/number of passes or for long times during HPH and US, respectively, that indeed do not fit with industrial needs, such as continuous/uninterrupted flow, low energy consumption, low operating and maintenance costs, reduced replacement of wearing parts. Moreover, it cannot be underestimated that high intensity HPH and US processing may be responsible for undesired temperature increase (Abbas et al., 2013), that could negatively affect the product sensory and healthy quality. Thus, the possibility to decrease the energy requirement associated with HPH and US appears a hot topic in the attempt to reduce processing costs as well as increase the sustainability of food productions.

The aim of this work was to study technological solutions for nanoemulsion preparation to improve

the homogenization process efficiency, while reducing the energy requirement and thus costs. To this purpose, a 15% (w/w) oil-in-water mixture containing 4.5% (w/w) of a blend of non-ionic surfactants (i.e., Tween 80 and Span 80 in 1:1 w/w ratio) was subjected to HPH and US that were provided in combination at low and medium energy density values. In particular, a single pass HPH, in the range of 20 to 100 MPa, was applied before or after 20 or 60 s US. Particle size distribution and mean diameter, viscosity and physical stability of the HPH-US and US-HPH treated samples were assessed and compared with those relevant to emulsions prepared by the application of individual HPH (up to 150 MPa; single or multiple passes) and US (up to 300 s), providing comparable or higher energy densities. This investigation is, to date, the first attempt to study the feasibility of HPH and US combined techniques in the light of reducing the energy requirement and costs associated with emulsification.

2. Materials and methods

2.1 Coarse emulsion preparation

The oil phase was prepared by dispersing 0.35% (w/w) sorbitan monooleate (Span 80, Tego SMO V, A.C.E.F. S.p.A., Florenzuola d'Arda - Piacenza, Italy) into commercial sunflower oil. The aqueous phase was prepared by mixing 2.03% (w/w) polyoxyethylene monooleate (Tween 80, Tween80®, Sigma Aldrich, Milano, Italy) with deionized water. The aqueous and oil phases were stirred separately at 20 °C for 30 min until the surfactants were completely dissolved. The coarse emulsion was prepared by mixing 17.05% (w/w) oil phase with 82.95% (w/w) aqueous phase using a high-speed blender (Polytron, PT 3000, Cinematica, Littau, Swiss) at 8000 rpm for 1 min. The surfactants concentration in the coarse emulsion was 4.50% (w/w). The coarse emulsion was divided into two aliquots; the first one was taken as a control, while the other one was immediately subjected to the homogenization processes.

2.2. Homogenization processes

2.2.1 High pressure homogenization (HPH)

A continuous lab-scale high-pressure homogenizer (Panda Plus 2000, GEA Niro Soavi, Parma, Italy) supplied with two Re+ type tungsten carbide homogenization valves, with a flow rate of 10 L/h, was used to treat 150 mL of coarse emulsion. The first valve was the actual homogenization stage and was set at increasing pressure up to 150 MPa. The second valve was set at the constant value of 5 MPa. Additional samples were prepared by subjecting the coarse emulsion to HPH for up to 5 successive passes at 120 MPa. At the exit of the homogenizer, after the final pass, the nanoemulsions were forced into a heat exchanger (GEA Niro Soavi, Parma, Italy) and cooled to 20 ± 2 °C.

2.2.2 High power ultrasound (US)

An ultrasonic processor (Hieschler Ultrasonics GmbH, mod. UP400S, Teltow, Germany) with a titanium horn tip diameter of 22 mm was used. The instrument operated at constant ultrasound amplitude and frequency of 100 μm and 24 kHz, respectively. Aliquots of 150 mL of coarse emulsion were introduced into 250 mL capacity (110 mm height, 60 mm internal diameter) glass vessels. The tip of the sonicator horn was placed in the centre of the solution, with an immersion depth in the fluid of 50 mm. The ultrasound treatments were performed up to 300 s. At the end of each treatment, samples were cooled to 20 ± 2 °C in an ice bath.

2.2.3 Combined HPH and US

The coarse emulsion (150 mL) was subjected to HPH before or after US. The time between the two treatments did not exceed 30 s. Homogenization pressure was set at 20, 50, 80 and 100 MPa, while US treatments were applied for 20 and 60 s. Samples were cooled to 20 ± 2 °C at the end of the second treatment. In particular, the nanoemulsions were forced into a heat exchanger (GEA Niro Soavi, Parma, Italy) or cooled in an ice bath, depending on the final treatment, i.e. HPH or US.

2.3 Sample storage

After preparation, the nanoemulsions were collected and stored at 4 °C for up to 15 days.

2.4. Temperature measurement

The sample temperature was measured just before and immediately after (i.e. before the cooling step) each treatment by a copper-constantan thermocouple probe (Ellab, Hillerød, Denmark) immersed in the fluid, connected to a portable data logger (mod. 502A1, Tersid, Milan, Italy). In addition, during US, the temperature was recorded as a function of time, by immersing (50 mm) the thermocouple tip in the fluid, half way between the sonotrode and the inside wall of the vessel.

2.5. Energy density

The energy density (E_v, MJ/m^3) transferred from the homogenization valve to the sample was determined as described by Stang et al. (2001), according to equation (1):

$$E_v = \Delta P \qquad (1)$$

where ΔP is the pressure difference operating at the nozzles.

The energy density transferred from the ultrasound probe to the sample was determined calorimetrically by recording the temperature (T, K) increase during the homogenization process (Mason, Lorimer, & Bates, 1999; Raso, Mañas, Pagàn, & Sala, 1999; Schubert et al., 2003). The following equation (2) was used:

$$E_v = \frac{mc_p(\partial T / \partial t)}{V} \times t \qquad (2)$$

where m is the sample mass (kg), c_p is the sample heat capacity (4.186 kJ/kg K), V is the sample volume (m^3), and t (s) is the duration of the emulsification procedure.

The energy density of multiple passes HPH and combined treatments was calculated as the sum of the energy density values of the corresponding single pass HPH or US plus HPH treatments.

2.6. Particle size distribution and particle size

The volume droplet size distribution of emulsions was measured by using the dynamic light scattering instrument Particle Sizer NICOMPTM 380 ZLS (PSS NICOMP Particle Sizing System, Santa Barbara, California, USA). Samples were diluted 1:1000 (v/v) with deionised water prior to the analysis to avoid multiple scattering effects. The angle of observation was 90°. Solution refractive index and viscosity were set at 1.333 and 1.0 cP, respectively, corresponding to the values of pure water at 20 °C. Particle volume distribution was calculated by NICOMP Distribution Analysis.

The droplet size was expressed as the Sauter diameter $d_{3,2}$ (Canselier et al., 2002):

$$d_{3,2} = \frac{\sum_i n_i d_i^3}{\sum_i n_i d_i^2} \qquad (3)$$

where n_i and d_i are the number and the diameter belonging to the i^{th} class, respectively.

2.7. Viscosity

Rheological determination was performed at 20 °C with a Stresstech Rheometer (Reologica Instruments AB, Lund, Sweden) using concentric cylinders geometry. The temperature control was obtained by using a circulating coolant connected to a thermostat. Experimental flow curves were obtained at shear rates ranging from 10 to 200 s^{-1}.

2.8. Stability

Emulsion stability was evaluated using a multisample analytical centrifuge (LUMiSizer, L.U.M. GmbH, Berlin, Germany). Nanoemulsions (0.4 mL) were transferred to rectangular polycarbonate cells (2 × 8 mm) and analysed by a light beam emitted at near infrared wavelength (865 nm) which scanned the sample cells over the entire sample length for a given time span. A charge coupled device (CCD) line sensor received the light transmitted through the sample. A pattern of light flux was obtained as a function of the sample radial position, giving a macroscopic fingerprint of the sample at a given time, from which emulsion instability, such as creaming or phase separation, can be assessed. In the current study, nanoemulsions were centrifuged at 4000 rpm and 20 °C at a scanning

rate of once every 30 s for 12000 s. The result was expressed as the integral transmission percentage, that represents the ratio of light transmitted from the sample, against time (Lerche & Sobish, 2007). The lower this value the greater the emulsion stability.

2.9. Data analysis

The results reported here are the average of at least three measurements carried out on two replicated experiments. Data are reported as mean value ± standard deviation. Statistical analysis was performed by using R v. 2.15.0 (The R foundation for Statistical Computing). Bartlett's test was used to check the homogeneity of variance, one way ANOVA was carried out and Tukey test was used to determine statistically significant differences among means ($p<0.05$).

3. Results and discussion

In this paper, the potential of applying combinations of high pressure homogenization (HPH) and high power ultrasound (US) treatments to obtain stable nanoemulsions, while minimizing the energy requirement was studied. To this purpose, an emulsion containing 15.0% (w/w) of sunflower oil and a 4.5% (w/w) mixture of Tween 80 and Span 80 (1:1 w/w) was considered. This emulsifier mixture was previously reported to form highly stable emulsions, due to the formation of a mixed layer of non-ionic surfactants on emulsion droplets (Lu & Rhodes, 2000; Berton, Genot, Guibert, & Ropers, 2012; Mosca, Cuomo, Lopez, & Ceglie, 2013). It is known that non-ionic emulsifiers, such as Tweens and Spans, rapidly absorb at the droplet surface during homogenization without undergoing structural modifications even when high homogenization energy is applied (Hayes, Fox, & Kelly, 2005; Ghosh, Mukherejee, & Chandrasekaran, 2013; Amani, York, Chrystin, & Clark, 2010). Preliminary trials showed that the emulsion formulation used in this study was performed well in terms of mean particle diameter.

Combinations of HPH (single pass, 20 to 100 MPa) and US (20 or 60 s), the ultrasonication being applied either before or after the HPH step, were performed. Contextually, HPH (1 pass up to 150

MPa, and multiple passes at 120 MPa) and US (up to 300 s) treatments were applied individually. Table 1 shows the maximum temperature, measured before the cooling step, and the energy density values of the samples subjected to HPH and US treatments, applied either individually or in combination. As already pointed out, the energy density of multiple passes or combined US and HPH was calculated as the sum of the energy densities supplied by the relevant single treatments. It is noteworthy that the energy density is an indicator of the treatment intensity, because it incorporates the transferred power, the duration of the treatment and the treated sample volume (Stang et al., 2001; Hulsmans et al., 2010). Temperature increased linearly (R^2>0.98, $p<0.05$) with the increasing of pressure or ultrasonication time, and never exceeded 53 °C and 90 °C during the HPH and US treatments, respectively. The energy densities transferred from the HPH valve and US probe into the fluid ranged between 20 MJ/m^3 and 600 MJ/m^3, depending on pressure and/or treatment time. From Table 1 it can be also observed that the combination of US and HPH at low pressure and short lengths of time allowed to obtain energy densities comparable to those generated by the application of intense individual US and HPH. For instance, an energy density of approximately 150 MJ/m^3 was obtained by applying 150 MPa, 120 s US, or 60 s US in combination with HPH at 80 MPa.

The effects of the homogenization treatments on the physical properties of emulsions were evaluated. Figs. 1 and 2 show the volume particle size distributions of emulsions obtained by means of individual and combined HPH and US, respectively. The coarse emulsion (data not shown) presented a bimodal distribution, showing a main broad peak (corresponding to 98% of the total particles) with a maximum at about 1000 nm and diameters ranging from 500 nm to 7000 nm, and a smaller peak at approximately 30 nm, with diameters ranging from 10 to 50 nm. By applying HPH and US treatments, a monomodal distribution was obtained in agreement with the literature (Floury et al., 2000; Cortèz-Munos et al., 2009). Moreover, the distribution width progressively decreased with increasing the treatment intensity, due to the disruption of particles with higher diameters (Canselier et al., 2002; Thiebaud, Dumay, Picart, Guiraud, & Cheftel, 2003). For comparable energy density values, the distribution width of emulsions obtained by the combined treatments was always lower than that of

241 samples prepared by applying the individual homogenization processes. For instance, 60 s US in
242 combination with HPH at 80 MPa provided the same energy density (*circa* 150 MJ/m^3) of single pass
243 HPH at 150 MPa or 120 s US; nevertheless, in the former case, a narrower distribution curve with a
244 maximum at a lower diameter value was obtained as respect to the individual treatments. In all cases,
245 the application of US before HPH resulted in a greater reduction of the distribution width (Fig. 2),
246 although this treatment required the same energy density as the HPH-US process.
247 The Sauter diameters $d_{3,2}$ of the samples subjected to HPH and US treatments are also shown in Table
248 1, to allow linking to the correspondent process parameters, e.g. pressure, number of passes, time, as
249 well as energy density values. The particle size values of emulsions obtained by US or HPH were in
250 the same order of magnitude as those reported in the literature for oil-in-water emulsions (Canselier
251 et al., 2002; Schubert et al., 2003). With reference to single pass HPH, emulsions mean particle
252 diameter significantly decreased with increasing the energy density up to 80 MJ/m^3, corresponding
253 to a pressure of 80 MPa, in agreement with literature results (Floury et al., 2000; Quian &
254 McClements, 2011; Tadros, Izquierdo, Esquena, & Solans, 2004). A further energy density increase,
255 provided by single pass HPH at pressure values up to 150 MPa, did not significantly modify the mean
256 diameter (p>0.05). It is likely that at these energy values, no further reduction of mean diameter was
257 observed because of the prevalence of coalescence events (McClements, 2011). Only by increasing
258 the number of consecutive passes through the valve from 1 to 5, leading to energy values up to 600
259 MJ/m^3, a significant further reduction (p<0.05) of the mean particle diameter was achieved, in
260 agreement with the literature (Floury et al., 2000; Thiebaud et al., 2003). Similarly, the particle size
261 mean diameter of emulsions obtained by US decreased with the increasing of the energy density to
262 approximately 143 MJ/m^3, while no more particle size reduction was achieved as the US energy
263 increased (p>0.05). These data are in agreement with previous studies (Ghosh et al., 2013; Leong et
264 al., 2009), showing that above a certain energy level cavitation becomes less efficient, possibly due
265 to the screening effect of cavitation bubbles crowding around the sonotrode surface. Table 1 also
266 shows that the combined HPH-US and US-HPH treatments led to mean particle diameters

significantly lower than those of individual US or HPH processes, provided the same energy density is imparted. This indicates that a significant reduction of the energy density can be achieved without losing in the effectiveness of the homogenization process. It can be noted that all the combined treatments allowed to obtain nanoemulsions, i.e. emulsions having diameter around 100 nm, even at low energy density values. From Table 1 it can be also observed that at low energy densities, when US preceded the HPH treatment, nanoemulsions had slight but significantly lower mean particle diameter than samples prepared by applying the HPH-US sequence ($p<0.05$).

The higher efficiency of the combined treatments in reducing the droplet dimensions (< 100 nm) as compared to the individual processes, could be attributed to an effect of the sequential application of the homogenization steps. It can be inferred that the first homogenization step would serve to reduce particle dimension and distribution width of the coarse emulsion (Figs 1 and 2), whose droplets were further broken in the second homogenization step, thus leading to a fine emulsion. In other words, as previously suggested (Pandolfe, 1995; Canselier at al., 2002; Abbas et al., 2013), the first homogenization step would improve the efficiency of the second homogenization step in obtaining particle diameter even lower. Moreover, an effect of treatment combination and sequence on chemical and physical properties of the mixed emulsifier layer adsorbed at the droplet surface could be assumed.

Fig. 3 shows the outcome of emulsion viscosity determinations. All samples showed Newtonian behaviour; however, differences were found among emulsions obtained by means of the different homogenization processes. The viscosity increased with the increasing of US energy density up to approximately 140 MJ/m^3. No further increase of this parameter was observed at higher energy density, probably due to excessive cavitation phenomena. No significant changes of sample viscosity were found by applying a single pass HPH for increasing pressures, although the treatment intensity increased. A significant increase in viscosity (from 2.19 x 10^{-3} to 4.78 x 10^{-3} Pa s) was obtained only by increasing the number of consecutive passes that corresponded to an increase in energy density up to 600 MJ/m^3 (Table 1). As shown in Fig. 3, the viscosities of samples subjected to HPH-US for

increasing energy densities were not significantly different, with a mean value of $2.4 \pm 0.2\ 10^{-3}$ Pa s. Similar data were obtained for the samples subjected to the US-HPH processes providing energy densities not exceeding 100 MJ/m^3. On the contrary, by applying this combined treatment with higher energy input (up to 175 MJ/m^3), a significant increase in viscosity was obtained. Data also show that emulsions prepared by means of multiple passes at 120 MPa showed viscosity values higher than emulsions obtained by applying the combined treatments, although the latter had lower particle size dimensions (Table 1, Figure 3). It can be inferred that, in our experimental conditions, the viscosity increase cannot be attributed only to a reduction of the particle diameter. An influence of particle surface properties on emulsion viscosity could be suggested.

The physical stability of the emulsions obtained by using HPH and US, applied either individually or in combination, was studied during storage at 4 °C for up to 15 days. No changes in the mean particle size were found as a function of storage time (data not shown), likely due to the low mean particle diameter of emulsions. Therefore, emulsion physical stability was evaluated by means of an accelerated creaming method. Fig. 4 shows the evolution of the integral transmission percentage of a selection of emulsions obtained by means of individual or combined US and HPH, using the analytical centrifuge; the corresponding energy density values are also reported. The lower the integral transmission value the greater the emulsion stability. The integral transmission greatly increased in the initial 6000 s for emulsions obtained by the application of treatments at low energy density, indicating fast creaming in these samples. By increasing the energy density, such an index increased less, suggesting higher stability of emulsions. However, as exemplified in Fig. 4, a higher stability did not always correspond to lower mean particle diameter. For instance, the emulsion subjected to 3 passes HPH (360 MJ/m^3) had higher stability and lower mean diameter particle (approx. 150 nm) than that obtained by the 60 s-80 MPa combined treatment (155 MJ/m^3, and Sauter diameter of 90 nm). The latter, in turn, showed higher stability than the correspondent reverse HPH-US process (155 MJ/m^3, mean particle diameter of 96 nm), although it imparted the same energy density, thus, confirming the greater efficiency of the US-HPH sequence as compared to the HPH-US treatments

in obtaining stable emulsions. Once again, results can be explained not only in terms of energy input but also assuming an influence of the homogenization process on the performances of the emulsifier blend.

4. Conclusions

Data acquired in this study clearly show that the combination of US with HPH was very advantageous to reduce the energy demand for emulsification. In particular, US and HPH provided in combination at low and medium energy density values allowed to obtain nanoemulsion having lower mean particle dimensions and, in most cases, higher stability than those prepared by using individual US or HPH at high energy density levels. Specifically, a greater efficiency was found for the US treatment preceding the HPH one.

From an industrial feasibility perspective, these results open new opportunities in the attempt to develop homogenization devices based on combined homogenization techniques. In fact, pressure (<60 MPa) and duration (a few s) requirements of the HPH and US combined processes are compatible with the industrial needs and could significantly contribute to reducing the total cost of ownership, thus leading to more sustainable treatments.

It is noteworthy that this technology has been performed on a model emulsion and tested on a laboratory scale. Therefore, further research has to be carried out to test the efficiency of the combined homogenization processes on systems different for composition and emulsifier characteristics from that used in the present study. Moreover, studies conducted at pilot and industrial scales represent a necessary task to develop a technology industrially exploitable.

References

Abbas, S., Hayat, K., Karangwa, E., Bashari, M., & Zhang, X. (2013). An overview of ultrasound assisted food-grade nanoemulsions. *Food Engineering Reviews, 5,* 139-157.

Amani, A., York, P., Chrystin, H., & Clark, B. (2010). Factors affecting stability of

345 nanoemulsions-use of artificial neural networks. *Pharmaceutical Research, 27,* 33-45.

346 Anese, M., Mirolo, G., Beraldo, P., & Lippe, G. (2013). Effect of ultrasound treatments of tomato
347 pulp on microstructure and lycopene *in vitro* bioaccessibility. *Food Chemistry, 136,* 458-463.

348 Ashokkumar, M. (2011). The characterization of acoustic cavitation bubbles-an overview.
349 *Ultrasonics Sonochemistry, 18,* 864-872.

350 Barba, F.J., Grimi, N., & Vorobiev, E. (2015). New approaches for the use of non-conventional
351 cell disruption technologies to extract potential food additives and nutraceuticals from microalgae.
352 *Food Engineering Reviews, 7,* 45-62.

353 Berton, C., Genot, C., Guibert, D., & Ropers, M.H. (2012). Effect of lateral heterogeneity in mixed
354 surfactant-stabilized interfaces on the oxidation of unsaturated lipids in oil-in-water emulsions.
355 *Journal of Colloid and Interface Science, 377,* 244-250.

356 Canselier, J.P., Delmas, H., Wilhelm, A.M., Abismaïl, B. (2002). Ultrasound emulsification. An
357 Overview. *Journal of Dispersion Science and Technology, 23,* 333-349.

358 Cortès-Muñoz, M., Chevalier-Lucia, D., & Dumay, E. (2009). Characteristic of submicron
359 emulsion prepared by ultra-high pressure homogenisation: Effect of chilled or frozen storage. *Food*
360 *Hydrocolloids, 23,* 640-654.

361 Delmas, T., Hin, P., Couffin, A.C., Texier, I., Fo, V., Poulin, P., et al. (2011). How to prepare and
362 stabilize very small nanoemulsions. *Langmuir, 27,* 1683-1692.

363 Donsì, F., Annunziata, M. & Ferrari, M. (2013). Microbial inactivation by high pressure
364 homogenization: Effect of the disruption valve geometry. *Journal of Food Engineering, 115,* 362-
365 370.

366 Dumay, E., Chevalier-Lucia, L., Benzaria, A., Gracià-Julià, A., & Blayo, C. (2013). Technological
367 aspects and potential applications of (ultra) high-pressure homogenization. *Trends in Food Science*
368 *and Technology, 31,* 13-26.

369 Fathi, M., Martin, A., & McClements, D.J. (2014). Nanoencapsulation of food ingredients using
370 carbohydrate based delivery systems. *Trends in Food Science & Technology, 39,* 18-39.

Floury, J., Bellettre, J., Legrand, J., & Desrumaux, A. (2004). Analysis of a new type of high pressure homogenizer. A study of the flow pattern. *Chemical Engineering Science, 59,* 843-853.

Floury, J., Desrumaux, A., & Lardiéres, J. (2000). Effect of high-pressure homogenization on droplet size distributions and rheological properties of model oil-in-water emulsions. *Innovative Food Science & Emerging Technologies, 1,* 127-134.

Floury, J., Desrumaux, A., & Legrand, J. (2002). Effect of ultra-high-pressure homogenization on structure and on rheological properties of soy protein-stabilized emulsions. *Journal of Food Science, 67,* 3388-3395.

Floury, J., Legrand, J., & Desrumaux, A. (2004). Analysis of a new type of high pressure homogeniser. Part B. Study of droplet break up and recoalescence phenomena. *Chemical Engineering Science, 59,* 1285-1294.

Freudig, B., Tesch, S., & Schubert, H. (2003). Production of emulsion in high-pressure homogenizers-Part II: Influence of cavitation on droplet breakup. *Engineering in Life Science, 3,* 266-270.

Ghosh V., Mukherejee A., & Chandrasekaran N. (2013). Ultrasonic emulsification of food-grade nanoemulsion formulation and evaluation of its bacterial activity. *Ultrasonics Sonochemistry, 20,* 338-344.

Hayes, M.G., Fox, P., & Kelly, A.L. (2005). Potential applications of high pressure homogenization in processing of liquid milk. *Journal of Diary Research, 72,* 25-33.

Huang, H.W., Hsu, C.P., Yang, B.B., & Wang, C.Y. (2013). Advances in the extraction of natural ingredients by high pressure extraction technology. *Trends in Food Science & Technology, 33,* 54-62.

Hulsmans, A., Joris, K., Lambert, N., Rediers, H., Declerk, P., & Delaedt, Y. (2010). Evaluation of process parameters of ultrasonic treatment of bacterial suspensions in a pilot scale water disinfection system. *Ultrasonic Sonochemistry, 17,* 1004-1009.

Jafari, S.M., He, Y., & Bhandari, B. (2006). Nano-emulsion production by sonication and

microfluidization-a comparison. *International Journal of Food Properties, 9*, 475-485.

Kentish, S., Wooster, T., Ashokkumar, M., Balachandran, S., Mawson, R., & Simons, L. (2008). The use of ultrasonics for nanoemulsion preparation. *Innovative Food Science and Emerging Technologies, 9,* 170-175.

Lee, L., & Norton, I.T. (2013). Comparing droplet breakup for a high pressure valve homogenizer and a microfluidizer for the potential production of food-grade nanoemulsions. *Journal of Food Engineering, 114,* 158-163.

Leong, T.S.H., Wooster, T.J., Kentish, S.E., & Ashokkumar, M. (2009). Minimizing oil droplet size using ultrasonic emulsification. *Ultrasonics Sonochemistry, 16,* 721-727.

Lerche, D., & Sobisch, T. (2007). Consolidation of concentrated dispersions of nano and microparticles determined by analytical centrifugation. *Powder Technology, 174,* 46-49.

Lu, D., & Rhodes, D.G. (2000). Mixed composition films of Spans and Tween 80 at the air-water interface. *Langmuir,16,* 8107-8112.

Mason, T.J, Lorimer, J.P., & Bates, D.M. (1999). Quantifying sonochemistry: casting some light on a "black art". *Ultrasonics, 30,* 40-42.

McClements J.M. (2011). Edible nanoemulsions: fabrication, properties, and functional performance. *Soft Matter, 7,* 2297-2316.

McClements, D.J. (2005). *Food Emulsions: Principle, Practice and Techniques* (2nd ed.), Boca Raton, FL: CRC Press.

Mosca, M., Cuomo, F., Lopea, F., & Ceglie, A. (2013). Role of emulsifier layer, antioxidants and radical initiators in the oxidation of olive oil-in-water emulsions. *Food Research International, 50,* 377-383.

Pandolfe, W.D. (1995). Effect of premix condition, surfactant concentration and oil level on the formation of oil-in-water emulsions by homogenization. *Journal of Dispersion Science and Technology, 16,* 633-650.

Panozzo, A., Lemmens, L., Van Loey, A., Manzocco, L., Nicoli, M.C., & Hendrickx, M. (2013).

Microstructure and bioaccessibility of different carotenoid species as affected by high pressure homogenization: A case study on differently coloured tomatoes. *Food Chemistry*, *141*, 4094-4100.

Patrignani, F., Vanni, L., Sado Kamdem, S., Hernando, I., Marco-Moles, R., Guerzoni, M. E., et al. (2013). High pressure homogenization vs heat treatment: Safety and functional properties of liquid whole egg. *Food Microbiology*, *36*, 63-69.

Quian, C., & McClements, D.J. (2011). Formation of nanoemulsions stabilized by model food-grade emulsifiers using high-pressure homogenization: Factors affecting particle size. *Food Hydrocolloids*, *25*, 1000-1008.

Raso, J., Manas, P., Pagan, R., & Sala, F.J. (1999). Influence of different factors on the output power transferred into medium by ultrasound. *Ultrasonics Sonochemistry*, *5*, 157-162.

Rastogi, N.K. (2011). Opportunities and challenges in application of ultrasound in food processing. *Critical Reviews in Food Science and Nutrition, 51,* 705-722

Schubert, H., Ax, K., & Behrend, O. (2003). Product engineering of dispersed systems. *Trends in Food Science & Technology*, *14*, 9-16.

Silva, H.D., Cerqueira, M.A., & Vicente, A.A. (2012). Nanoemulsions for food applications: development and characterization. *Food and Bioprocess Technology, 5*, 854-867.

Solans C., Izquierdo, P., Nolla, J., Azemar, N., & Garcia-Celma, N.J. (2005). Nano-emulsion. *Current Opinion in Colloid & Interface Science, 10,* 102-110.

Stang, M., Schschmann, H., & Schubert, H. (2001). Emulsification in high-pressure homogenizers. *Engineering in Life Science, 1*, 151-157.

Tadros, T.F., Izquierdo, P., Esquena, J., & Solans, C. (2004). Formation and stability of nano-emulsions. *Advances in Colloid and Interface Science, 108-109*, 303–318.

Thiebaud, M., Dumay, E., Picart, L., Guiraud, J.P., & Cheftel, J.C. (2003). High-pressure homogenisation of raw bovine milk. Effects on fat globule size distribution and microbial inactivation. *International Dairy Journal, 13*, 427-439.

Figure captions

Fig. 1. Volume particle size distribution of emulsions obtained by application of HPH (a) and US (b).

Fig. 2. Volume particle size distribution of emulsions obtained by application of combined HPH and US. HPH at 20 and 80 MPa was applied either before or after 20 s (a) or 60 s (b) US.

Fig. 3. Viscosity of emulsions obtained by US and HPH, applied either individually or in combination, as a function of energy density.

Fig. 4. Integral transmission percentage of emulsions obtained by HPH and US, applied either individually or in combination, as a function of centrifugation time.

Table 1

Temperature (± standard deviation), energy density and particle diameter (± standard deviation) of emulsions subjected to HPH and US provided individually or in combination. Starting temperature, 20 ± 2 °C.

Treatment	Pressure (MPa)	Number of passes	Time (s)	Temperature* (°C)	Energy density (MJ/m^3)	Sauter diameter (nm)
HPH	20	1		22.1 ± 0.5	20	291 ± 55^{a}
	50	1		24.6 ± 0.4	50	288 ± 37^{a}
	80	1		30.8 ± 0.4	80	196 ± 32^{ab}
	100	1		33.5 ± 0.3	100	173 ± 7^{ab}
	120	1		37.6± 0.5	120	167 ± 14^{ab}
	150	1		42.5 ± 0.6	150	185 ± 15^{ab}
	120	3		48.6 ± 0.6	360	151 ± 3^{ab}
	120	5		52.5 ± 0.6	600	121 ± 8^{b}
US			20	28.2 ± 0.5	28	304 ± 50^{a}
			30	31.4 ± 0.5	40	242 ± 2^{ab}
			40	34.9 ± 0.3	52	187 ± 41^{ab}
			60	41.6 ± 0.4	75	151 ± 2^{b}
			120	60.9 ± 0.3	143	125 ±2^{b}
			300	89.9 ± 0.2	348	112 ± 8^{b}
US-HPH	20	1	20		48	98 ± 6^{a}
	50	1	20		78	101 ± 2^{a}
	80	1	20		108	90 ± 2^{a}
	100	1	20		128	96 ± 4^{a}
	20	1	60		95	91 ± 6^{a}
	50	1	60		125	92 ± 4^{a}
	80	1	60		155	90 ± 3^{a}
	100	1	60		175	93 ± 6^{a}
HPH-US	20	1	20		48	121 ± 4^{a}
	50	1	20		78	110 ± 2^{ab}
	80	1	20		108	106 ± 1^{ac}
	100	1	20		128	88 ± 8^{c}
	20	1	60		95	101 ± 2^{ac}
	50	1	60		125	105 ± 1^{ac}
	80	1	60		155	96 ± 1^{bc}
	100	1	60		175	90 ± 4^{bc}

*Temperature was measured at the end of each treatment, just before the cooling step.

$^{a\text{-}c}$ within each treatment, means with different letters are significantly different ($p<0.05$)

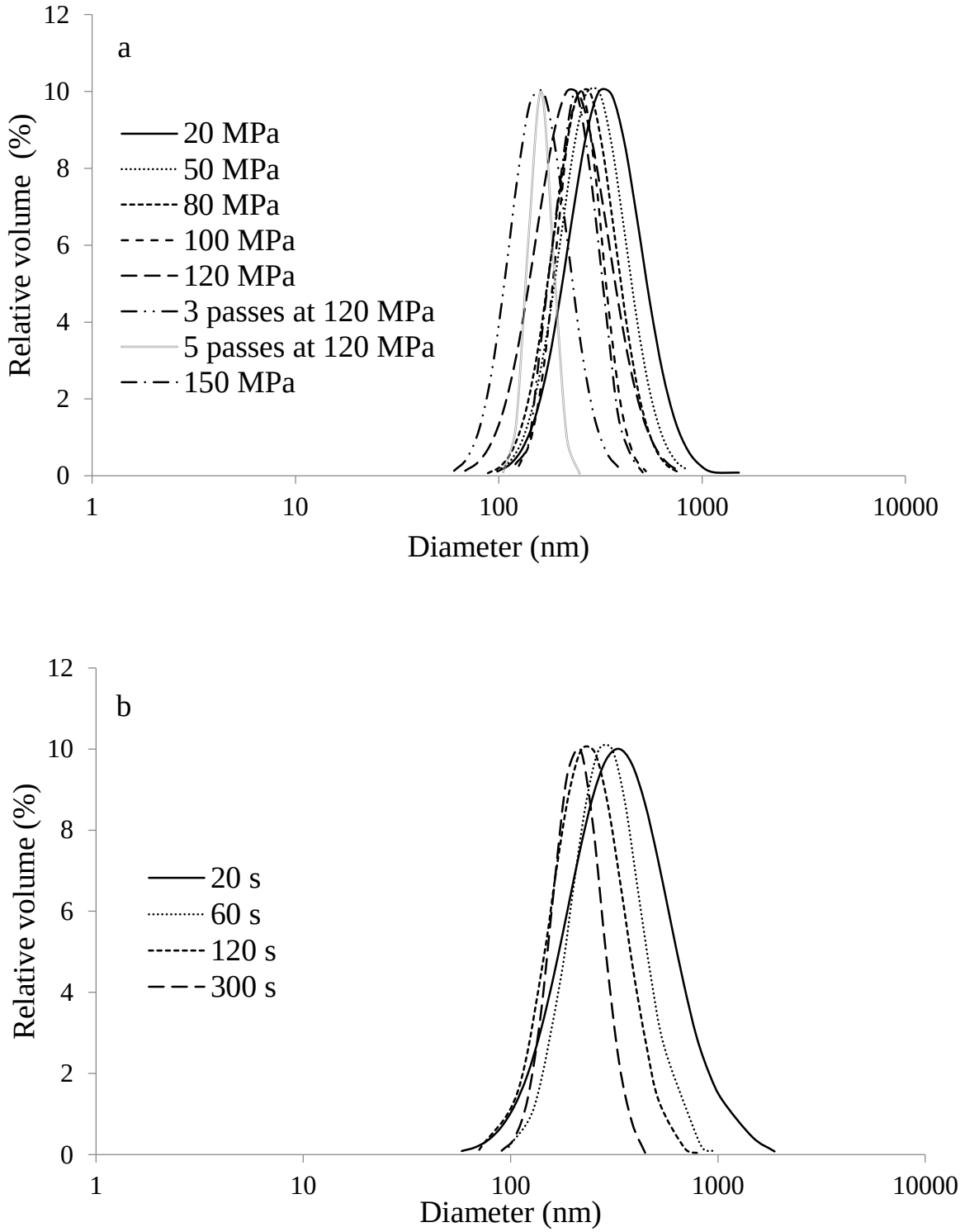
a
Relative volume (%)
Diameter (nm)
20 MPa
50 MPa
80 MPa
100 MPa
120 MPa
3 passes at 120 MPa
5 passes at 120 MPa
150 MPa
b
Relative volume (%)
Diameter (nm)
20 s
60 s
120 s
300 s

Fig. 1.

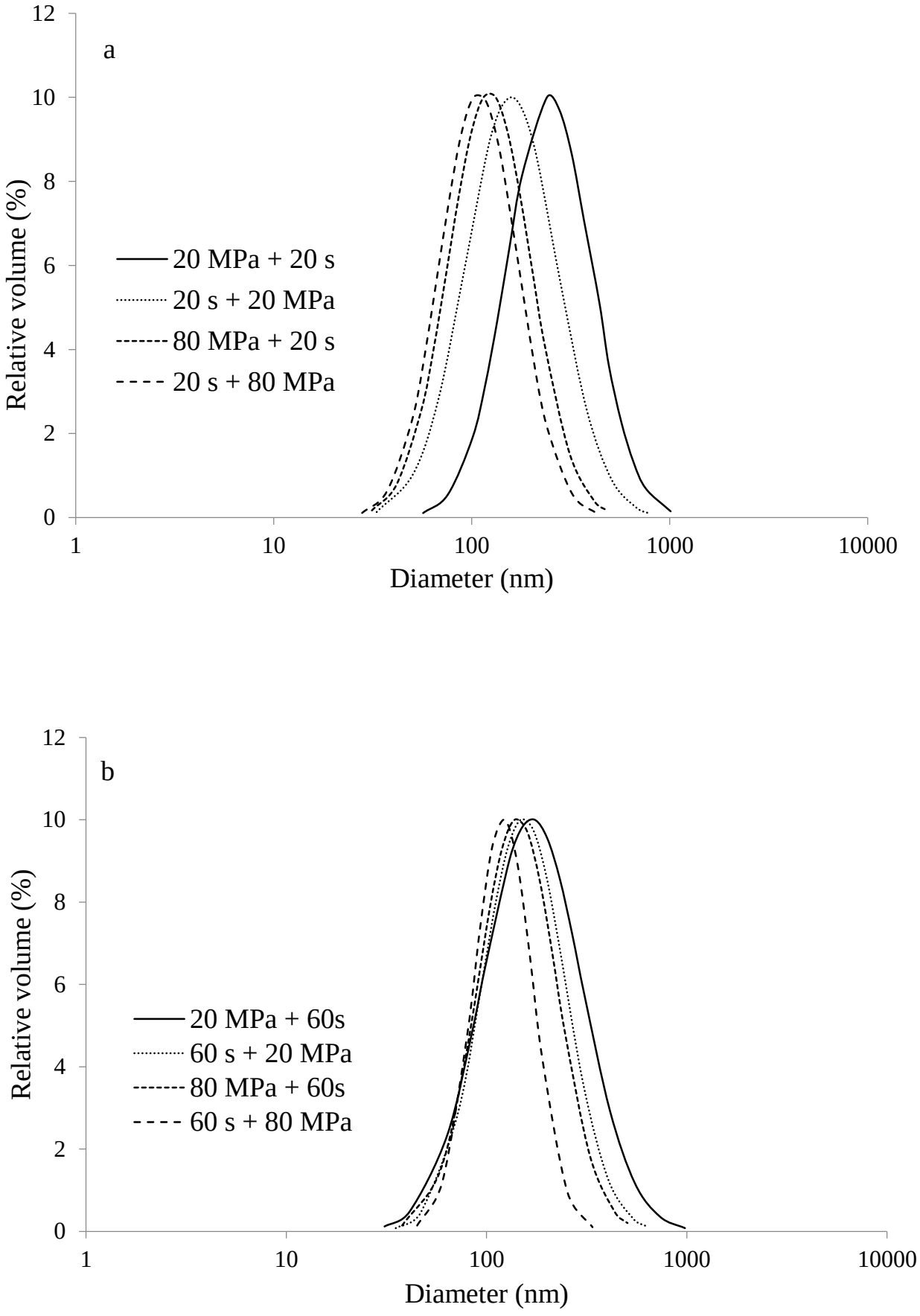
a
Relative volume (%)
Diameter (nm)
20 MPa + 20 s
20 s + 20 MPa
80 MPa + 20 s
20 s + 80 MPa
b
Relative volume (%)
Diameter (nm)
20 MPa + 60s
60 s + 20 MPa
80 MPa + 60s
60 s + 80 MPa

Fig. 2.

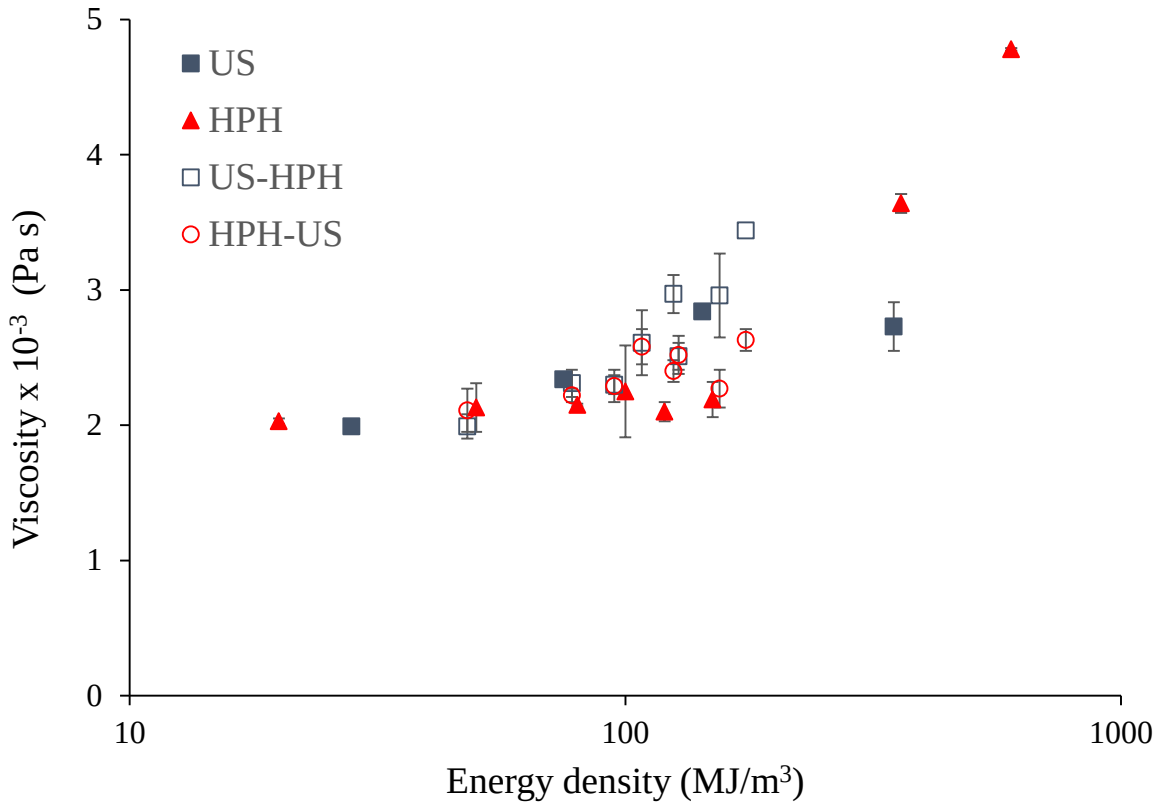
US
HPH
US-HPH
HPH-US
Viscosity x 10-3 (Pa s)
Energy density (MJ/m3)
0
1
2
3
4
5
10
100
1000

Fig. 3.

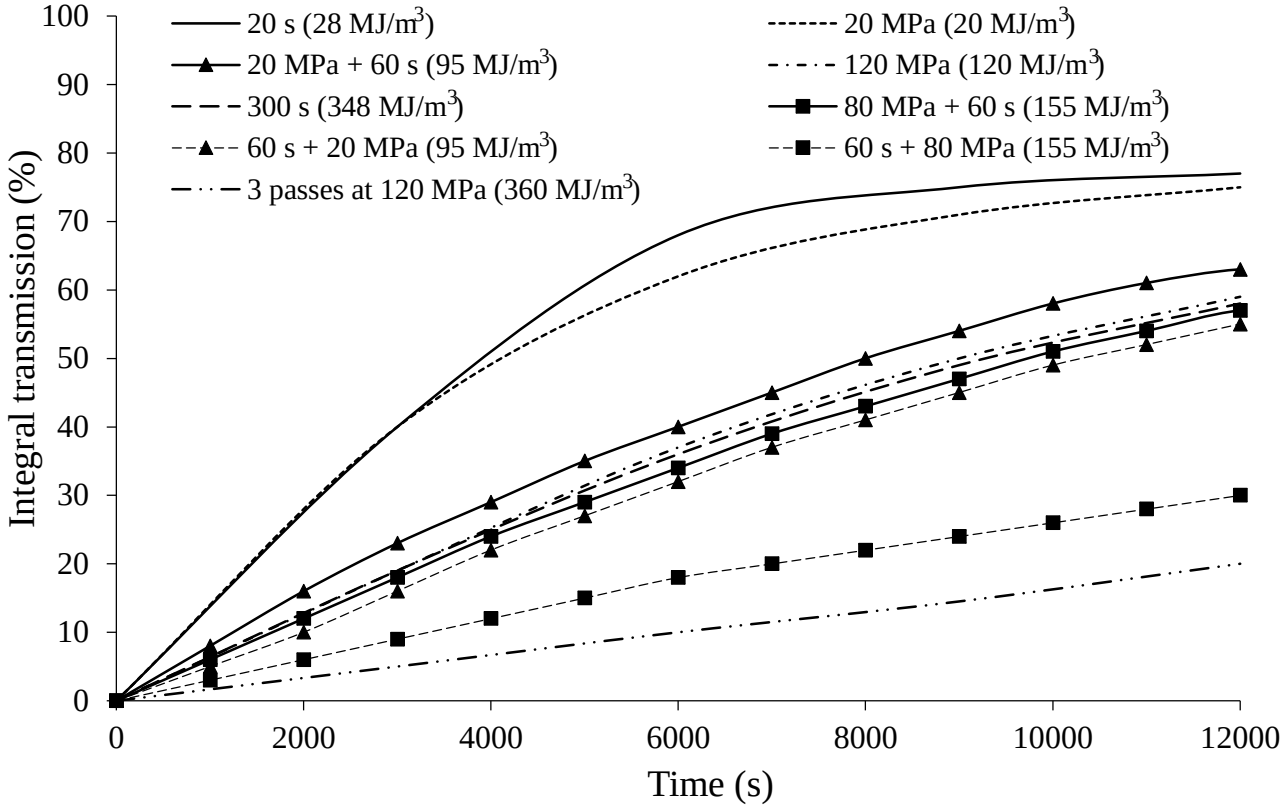
20 s (28 MJ/m3)
20 MPa (20 MJ/m3)
20 MPa + 60 s (95 MJ/m3)
120 MPa (120 MJ/m3)
300 s (348 MJ/m3)
80 MPa + 60 s (155 MJ/m3)
60 s + 20 MPa (95 MJ/m3)
60 s + 80 MPa (155 MJ/m3)
3 passes at 120 MPa (360 MJ/m3)
Integral transmission (%)
Time (s)
0
10
20
30
40
50
60
70
80
90
100
0
2000
4000
6000
8000
10000
12000

Fig. 4.